Supporting information

Pentacarbonitrile-based Efficient Near-Infrared Thermally Activated Delayed Fluorescence OLEDs via Suppressing Excited-State Structural Relaxation

Shengkai Hu,[a] Yang Li,[a] Kai Zhang,*[b] Dong-Ying Zhou,*[a] Liang-Sheng Liao,[a] and Jian Fan*[ac]

[a] *Institute of Functional Nano & Soft Materials (FUNSOM), Jiangsu Key Laboratory for Carbon-Based Functional Materials & Devices, Soochow University, Suzhou, Jiangsu 215123, China*

[b] *College of Physics and Engineering, Qufu Normal University, Qufu, Shandong 273165, China*

[c] *State Key Laboratory of Structural Chemistry, Fujian Institute of Research on Structure of Matter, Chinese Academy of Sciences, Fuzhou, Fujian 35002, China*

E-mail: 15692312996@163.com, dyzhou@suda.edu.cn, jianfan@suda.edu.cn

General Information

Materials

All commercially available reagents were used as received unless otherwise stated. All reactions were carried out using Schlenk techniques under a nitrogen atmosphere. ^{1}H NMR spectra were measured on a Bruker 400 MHz spectrometer with tetramethylsilane (TMS) as the internal standard. Mass analyses were recorded by an Auto flex MALDI-TOF mass spectrometer.

Thermal properties.

Thermogravimetric analysis (TGA) was performed on a TA SDT 2960 instrument at a heating rate of 10 ℃ min^{-1} under nitrogen. Temperature at 5% weight loss was used as the decomposition temperature (T_d).

Cyclic voltammetry measurements.

Cyclic voltammetry (CV) was carried out on a CHI600 voltammetric analyzer at

room temperature with ferrocenium-ferrocene (Fc^+/Fc) as the external standard. The oxidative scans were performed using 0.1 M *n*-Bu_4NPF_6 ($TBAPF_6$) in deoxygenated dichloromethane as the supporting electrolyte. A conventional three-electrode configuration consisting of a Pt-wire counter electrode, an Ag/AgCl reference electrode, and a Glassy-Carbon working electrode was used. The cyclic voltammograms were obtained at a scan rate of 0.1 V s^{-1}.

Calculation formulas for the photophysical parameters

$$k_F = \Phi_F/\tau_F$$

$$\Phi_{PL} = k_F/(k_F + k_{IC})$$

$$\Phi_F = k_F/(k_F + k_{IC} + k_{ISC})$$

$$\Phi_{ISC} = k_{ISC}/(k_F + k_{IC} + k_{ISC})$$

$$k_{TADF} = \Phi_{TADF}/(\Phi_{ISC}\tau_{TADF})$$

$$k_{RISC} = k_F k_{TADF}\Phi_{TADF}/(k_{ISC}\Phi_F)$$

$$\Phi_{TADF}/\Phi_F = (\Phi_{ISC}\Phi_{RISC})/(1 - \Phi_{ISC}\Phi_{RISC})$$

$\mathbf{\Phi_{PL}}$ is the total fluorescence quantum yield; $\mathbf{\Phi_F}$ is the prompt fluorescent component of $\mathbf{\Phi_{PL}}$; $\mathbf{\Phi_{TADF}}$ is the delayed fluorescent component of $\mathbf{\Phi_{PL}}$; $\mathbf{\tau_F}$ is the lifetime of prompt fluorescent; $\mathbf{\tau_{TADF}}$ is the lifetime of TADF; $\mathbf{k_F}$ is the rate constant of fluorescent; $\mathbf{k_{IC}}$ is the rate constant of internal conversion; $\mathbf{k_{TADF}}$, $\mathbf{k_{ISC}}$, $\mathbf{k_{RISC}}$ are the rate constants of TADF, intersystem crossing and reverse intersystem crossing, respectively; $\mathbf{\Phi_{ISC}}$ and $\mathbf{\Phi_{RISC}}$ are the quantum efficiencies of ISC and RISC process, respectively.

Photophysical measurements.

UV–Vis absorption spectra were recorded on a Hitachi U-3900 spectrophotometer. PL spectra and phosphorescent spectra were recorded on a Hitachi F-4600 fluorescence spectrophotometer. PL spectra were recorded on a Hitachi F-4600 fluorescence spectrophotometer with default collection intervals. Transient fluorescence decays in films were tested using Edinburgh Instruments FLS980 spectrometer. The absolute PL quantum yields were recorded on a Hamamatsu Quantaurus-QY quantum yield spectrometer (C13534-11).

Theoretical calculation

The polarized continuum model (PCM) method is used to evaluate the photophysical properties of TPA-5CN and TPA-2N in toluene. For the quantum mechanics calculations, the optimization followed the restricted Kohn−Sham (KS) DFT process, while for singlet excited state, the time-dependent density functional theory

(TD-DFT) optimizations are carried out using the restricted KS determinant as reference. In addition, unrestricted KS (UKS) ground state calculations are performed to study the triplet excited state. The PBE0-1/3 is adopted in all the following quantum mechanics calculations in the work. Besides, the 6-31G* basis set is used. All the calculations above are carried out in the Gaussian 16 package.[1] In addition, the transition dipole moment vector is achieved using the wave function analysis software Multiwfn.[2] The normal mode reorganization energies is achieved using the MOMAP (Molecular Materials Property Prediction Package) program.

Device fabrication and measurement of EL characteristics

The OLEDs were prepared with the configuration of ITO/HAT-CN(10 nm)/TAPC(50 nm)/TCTA(10 nm)/CBP: dopant (1-10 wt%) (20 nm)/B4PyMPM (65 nm)/Liq(2 nm)/Al(100 nm). The ITO glass substrates were degreased ultrasonically in alternate baths of alcohol and de-ionized water; then they were dried in an oven and treated by ultraviolet ozone for 15 minutes. Finally, followed by being loaded into an evaporator, the devices were fabricated under a high vacuum of 4×10^{-6} Torr. The evaporation rates were controlled with oscillating quartz crystals. The deposition rates are 0.5-2 Å s^{-1} for transporting organic layers, 0.02-0.1 Å s^{-1} for ultrathin emitting layers, 0.1 Å s^{-1} for Liq layer and 3-6 Å s^{-1} for Al cathode film, respectively. The current-voltage characteristics were measured with a computer-controlled Keithley 2400 source meter. Electroluminescence spectra were measured with a Photo Research SpectraScan PR 745 Photometer, which can detect spectral region of 380-1080 nm. All the measurements were carried out under ambient atmosphere at room temperature. The EQE values are calculated on the assumption of a Lambertian angular distribution of the EL intensity.

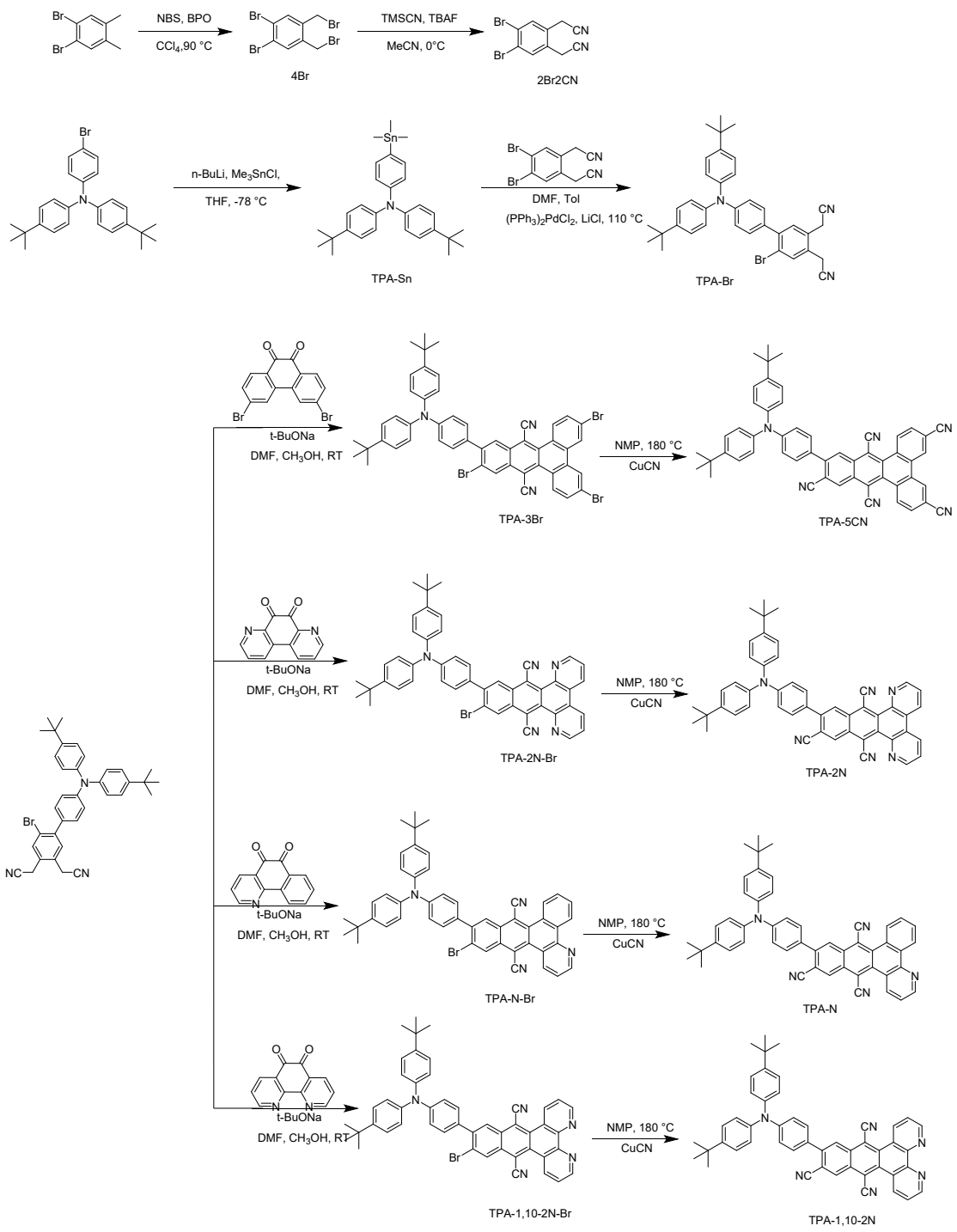

Scheme S1. Synthetic route of TPA-5CN, TPA-2N, TPA-N and TPA-1,10-2N.

1,2-dibromo-4,5-bis(bromomethyl)benzene (4Br)

1,2-Dibromo-4,5-dimethylbenzene (4.1 g, 15.53 mmol), NBS (6.08 g, 34.16 mmol), and BPO (188 mg, 0.78 mmol) were added to anhydrous CCl_4 (50 mL). The reaction mixture was stirred at 90 ℃ for 3 hours. After cooling down to room temperature, the precipitate was removed by filtration and the filtrated was washed with water (3 × 20 mL) and extracted with dichloromethane (3 × 20 mL). The combined organic portions were dried over anhydrous $MgSO_4$. The organic solvent was removed under reduced pressure, and the residue was purified by column chromatography on silica gel with hexane as eluent to give 4Br (6.1 g, 93%) as a white solid.^{1}H NMR (400 MHz, $CDCl_3$) δ 7.62 (s, 2H), 4.53 (s, 4H).

2,2'-(4,5-dibromo-1,2-phenylene)diacetonitrile (2Br2CN)

To a solution of 4Br (3.17 g, 7.6 mmol) in MeCN (30 mL), TMSCN (2.67 mL, 21.33 mmol) was added at 0 ℃. After stirring for 5 minutes, TBAF (21 mL, 1M in THF, 21 mmol) was added dropwise. The mixture was allowed to warm to room temperature and stirred for 24 h at N_2. After the removal of MeCN, the residue was extracted with DCM and dried over $MgSO_4$. The crude compound was purified by column chromatography on silica gel (hexane/EA = 3:1) to give 2Br2CN (820 mg, 38%) as a light yellow solid. ^{1}H NMR (400 MHz, $CDCl_3$) δ 7.72 (s, 2H), 3.72 (s, 4H).

4-(tert-butyl)-N-(4-(tert-butyl)phenyl)-N-(4-(trimethylstannyl)phenyl)aniline (TPA-Sn)

To a solution of 4-bromo-N,N-bis(4-(tert-butyl)phenyl)aniline (4 g, 9.17 mmol) in THF (40 mL), n-BuLi (5.5 mL, 2.5 M in THF, 13.76 mmol) was added at -78 ℃ under N_2. After stirring for 4 hours, Me_3SnCl (13.76 mL, 1 M in THF, 13.76 mmol) was added into the reaction mixture. After stirring for at room temperature for 24 hours, the reaction was quenched with H_2O and extracted with DCM. After the removal of organic solvent, the crude product was used in the next step without any further purification (3.8 g, 80%).

2,2'-(4'-(bis(4-(tert-butyl)phenyl)amino)-6-bromo-[1,1'-biphenyl]-3,4-diyl)diacetonitrile (TPA-Br)

2Br2CN (1 g, 3.18 mmol), TPA-Sn (1.66 g, 3.19 mmol), $(PPh_3)_2PdCl_2$(223 mg, 0.32 mmol), and LiCl (669 mg, 15.93 mmol) were added into a mixture of toluene (25 mL)/DMF(5 mL) under nitrogen. The mixture was stirred at 110 ℃ overnight. After cooling to room temperature, the precipitate was removed by filtration. The reaction mixture was diluted with water (20 mL) and extracted with dichloromethane (3 × 20 mL). The solvent was removed under reduced pressure, and the residue was purified by column chromatography on silica gel (hexane/EA = 3:1) to give TPA-Br (350 mg, 19%) as a yellow solid. ^{1}H NMR (400 MHz, $CDCl_3$) δ 7.74 (s, 1H), 7.43 (s, 1H), 7.34-7.28 (m, 4H), 7.25-7.20 (m, 2H), 7.13-7.04 (m, 6H), 3.76 (d, J = 6.8 Hz, 4H), 1.33 (s, 18H).

11-(4-(bis(4-(tert-butyl)phenyl)amino)phenyl)-3,6,12-tribromobenzo[f]tetraphene-9,14-dicarbonitrile (TPA-3Br)

To a solution of TPA-Br (600 mg, 1.02 mmol) and 3,6-dibromophenanthrene-9,10-dione (372 mg, 1.02 mmol) in DMF (30 mL), *t*-BuNa (146 mg, 1.52 mmol) was added in small portions. The reaction mixture was stirred at room temperature for 2.5 h. After quenching with excess water, a green solid was isolated by filtration and was used in the next step without any further purification due to the poor solubility (800 mg, 85.5%).

12-(4-(bis(4-(tert-butyl)phenyl)amino)phenyl)benzo[f]tetraphene-3,6,9,11,14-pentacarbonitrile (TPA-5CN)

CuCN (311 mg, 3.47 mmol) and TPA-3Br (800 mg, 0.87 mmol) were added into anhydrous NMP (30 mL). The reaction mixture was stirred at 180 ℃ for 48 h under N_2. After cooling to room temperature, the mixture was washed with aqueous $FeCl_3$. The precipitate was collected by filtration and washed with water. The crude product was purified by column chromatography on silica gel with DCM to give TPA-5CN (200 mg, 30%) as a green solid. ^{1}H NMR (400 MHz, $CDCl_3$,): δ 9.51 (dd, J = 8.3, 3.4 Hz,

2H), 9.10 (s, 1H), 8.81 (s, 2H), 8.68 (s, 1H), 8.09-8.02 (m, 2H), 7.62 (d, J = 8.5 Hz, 2H), 7.39 -7.32 (m, 4H), 7.22-7.12 (m, 6H). MALDI-TOF-MS: m/z calcd for $C_{53}H_{38}N_6$: 758.316, found: 758.298.

11-(4-(bis(4-(tert-butyl)phenyl)amino)phenyl)-12-bromonaphtho[2,3-f][4,7]phenanthroline-9,14-dicarbonitrile (TPA-2N-Br)

TPA-2N-Br was prepared with the similar procedure of TPA-3Br (600 mg, 66%).

12-(4-(bis(4-(tert-butyl)phenyl)amino)phenyl)naphtho[2,3-f][4,7]phenanthroline-9,11,14-tricarbonitrile (TPA-2N)

TPA-2N was prepared with the similar procedure of TPA-5CN as a black solid (180 mg, 32%). ^{1}H NMR (400 MHz, $CDCl_3$) δ 9.33 (s, 1H), 9.21 – 9.14 (m, 2H), 8.93 (s, 1H), 8.84 (d, *J* = 8.5 Hz, 2H), 7.84 (d, *J* = 8.7 Hz, 2H), 7.66 (d, *J* = 7.2 Hz, 2H), 7.35 (d, *J* = 7.8 Hz, 4H), 7.18 (dd, *J* = 14.2, 7.6 Hz, 6H). MALDI-TOF-MS: m/z calcd for $C_{53}H_{38}N_6$: 710.316, found: 710.297.

11-(4-(bis(4-(tert-butyl)phenyl)amino)phenyl)-12-bromobenzo[h]naphtho[2,3-f]quinoline-9,14-dicarbonitrile (TPA-N-Br)

TPA-N-Br was prepared with the similar procedure of TPA-3Br as a red solid (360 mg, 66%). ^{1}H NMR (400 MHz, $CDCl_3$) δ 9.74 (ddd, J = 8.4, 3.2, 1.5 Hz, 1H), 9.42 (ddd, J = 8.1, 3.3, 1.3 Hz, 1H), 9.31 – 9.24 (m, 1H), 9.04 (dd, J = 4.4, 1.5 Hz, 1H), 8.96 (d, J = 14.2 Hz, 1H), 8.55 (d, J = 14.5 Hz, 1H), 7.92 – 7.78 (m, 2H), 7.65 (dt, J = 8.7, 4.5 Hz, 1H), 7.48 – 7.39 (m, 2H), 7.38 – 7.30 (m, 4H), 7.21 – 7.11 (m, 6H), 1.35 (s, 18H).

11-(4-(bis(4-(tert-butyl)phenyl)amino)phenyl)benzo[h]naphtho[2,3-f]quinoline-9,12,14-tricarbonitrile (TPA-N)

TPA-N was prepared with the similar procedure of TPA-5CN as a red solid (210 mg, 75.3%). ^{1}H NMR (400 MHz, $CDCl_3$) δ 9.75 (ddd, *J* = 8.5, 3.5, 1.5 Hz, 1H), 9.46 – 9.39 (m, 1H), 9.29 (dt, *J* = 7.8, 2.0 Hz, 1H), 9.12 – 9.03 (m, 2H), 8.67 (d, *J* = 14.0 Hz,

1H), 7.89 (dtdd, *J* = 22.6, 7.6, 5.6, 1.6 Hz, 2H), 7.67 (ddd, *J* = 8.5, 4.4, 2.7 Hz, 1H), 7.62 (dd, *J* = 8.7, 1.8 Hz, 2H), 7.39 – 7.30 (m, 4H), 7.23 – 7.13 (m, 6H), 1.35 (s, 18H).

11-(4-(bis(4-(tert-butyl)phenyl)amino)phenyl)-12-bromonaphtho[2,3-f][1,10]phenanthroline-9,14-dicarbonitrile (TPA-1,10-2N-Br)

TPA-1,10-2N-Br was prepared with the similar procedure of TPA-3Br as a red solid (260 mg, 50%). ^{1}H NMR (400 MHz, $CDCl_3$) δ 9.86 (ddd, *J* = 8.5, 3.2, 1.5 Hz, 2H), 9.27 (dd, *J* = 4.4, 1.5 Hz, 2H), 9.01 (s, 1H), 8.58 (s, 1H), 7.80 (dt, *J* = 8.8, 4.6 Hz, 2H), 7.49 – 7.40 (m, 2H), 7.38 – 7.32 (m, 4H), 7.20 – 7.11 (m, 6H), 1.34 (s, 18H).

12-(4-(bis(4-(tert-butyl)phenyl)amino)phenyl)naphtho[2,3-f][1,10]phenanthroline-9,11,14-tricarbonitrile (TPA-1,10-2N)

TPA-1,10-2N was prepared with the similar procedure of TPA-5CN as a red solid (140 mg, 47.1%). ^{1}H NMR (400 MHz, $CDCl_3$) δ 9.86 (ddd, *J* = 8.5, 2.8, 1.5 Hz, 2H), 9.30 (td, *J* = 4.1, 1.4 Hz, 2H), 9.12 (s, 1H), 8.71 (s, 1H), 7.82 (ddd, *J* = 8.5, 4.4, 2.6 Hz, 2H), 7.66 – 7.58 (m, 2H), 7.40 – 7.32 (m, 4H), 7.21 – 7.08 (m, 6H), 1.35 (s, 17H).

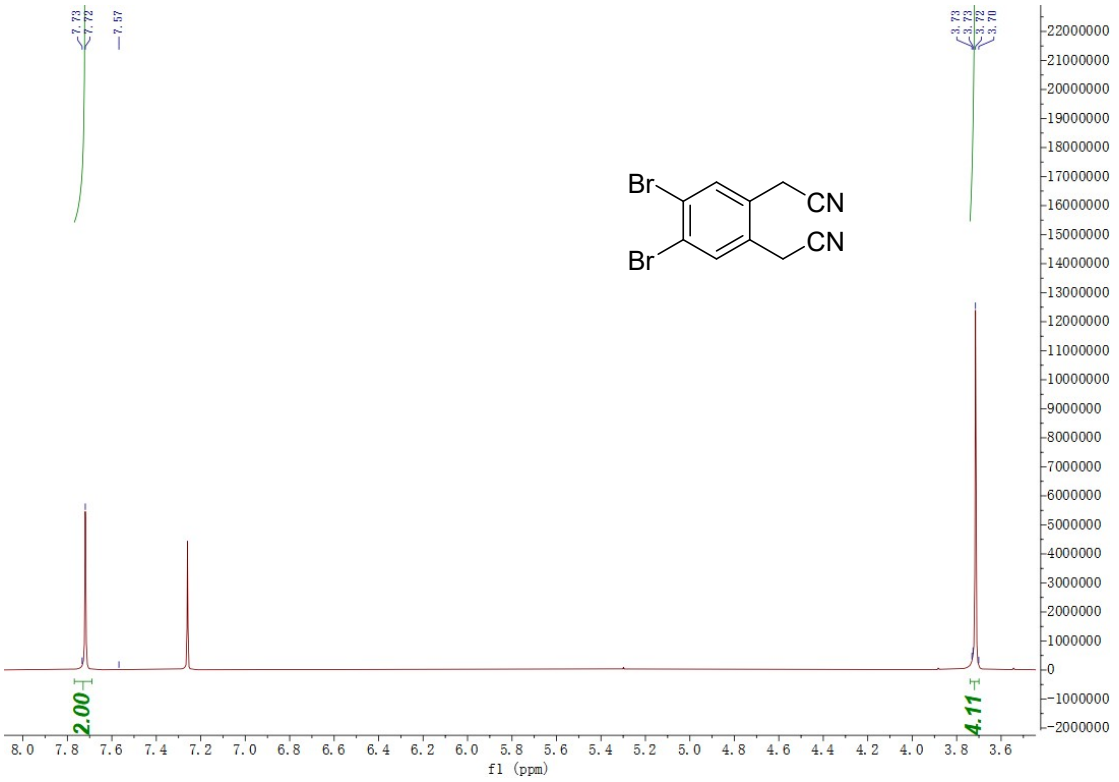

Figure S1 ^{1}H NMR spectrum ($CDCl_3$, 400 MHz) of 2Br-2CN.

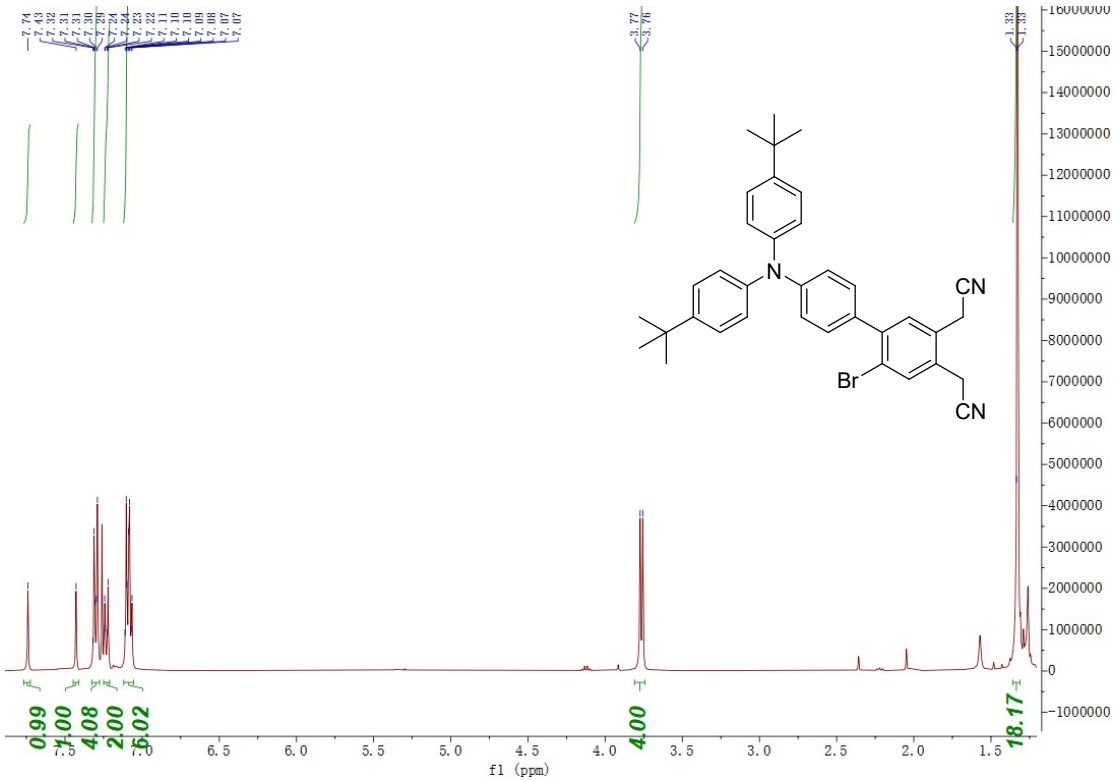

Figure S2 ^{1}H NMR spectrum ($CDCl_3$, 400 MHz) of TPA-3Br.

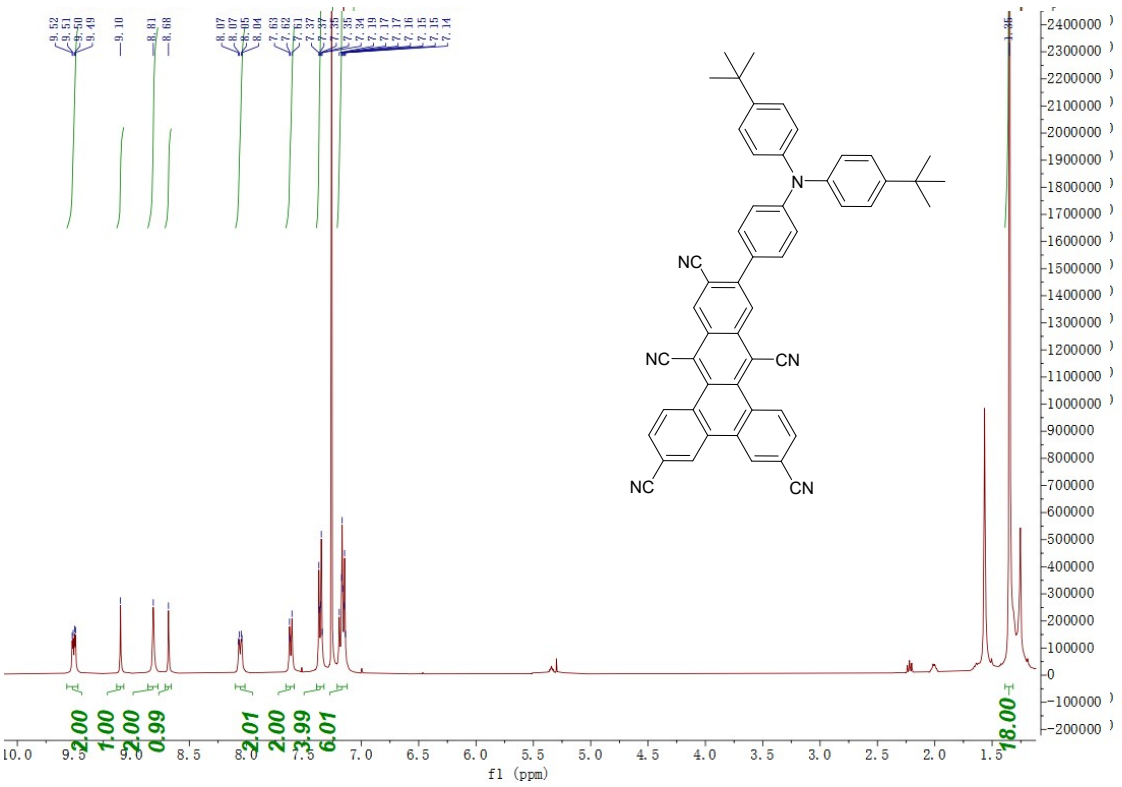

Figure S3 ^{1}H NMR spectrum ($CDCl_3$, 400 MHz) of TPA-5CN.

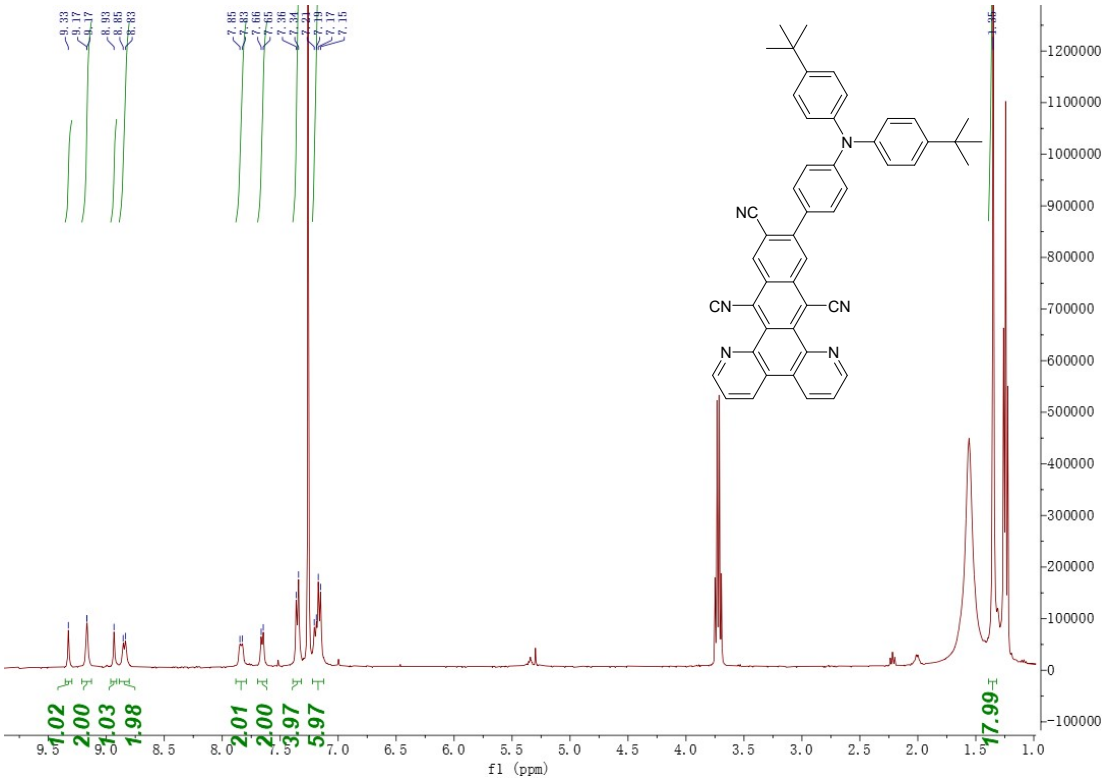

Figure S4 ^{1}H NMR spectrum ($CDCl_3$, 400 MHz) of TPA-2N.

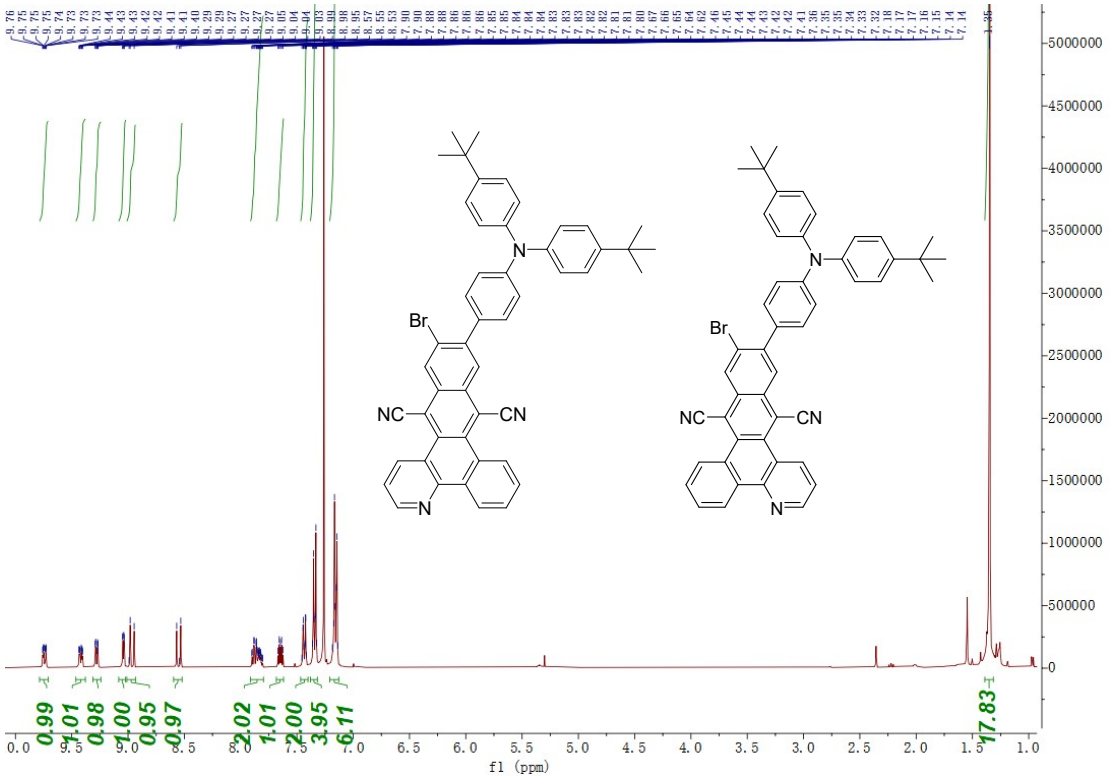

Figure S5 ^{1}H NMR spectrum ($CDCl_3$, 400 MHz) of TPA-N-Br.

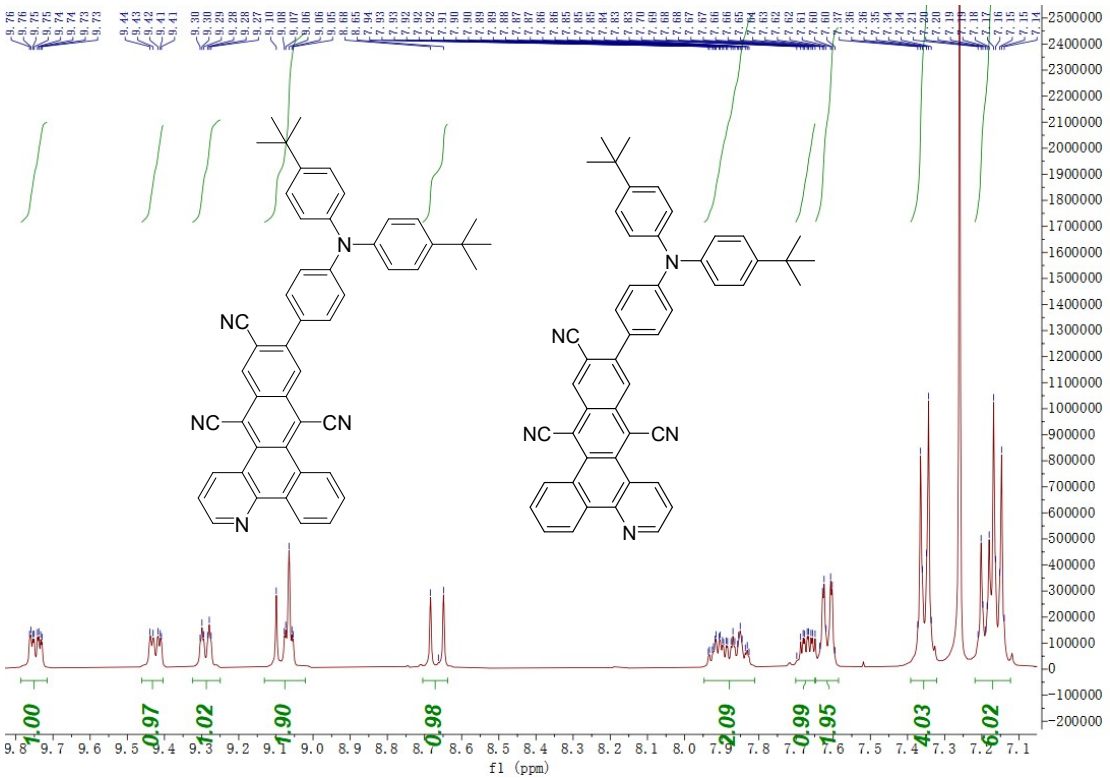

Figure S6 ^{1}H NMR spectrum ($CDCl_3$, 400 MHz) of TPA-N.

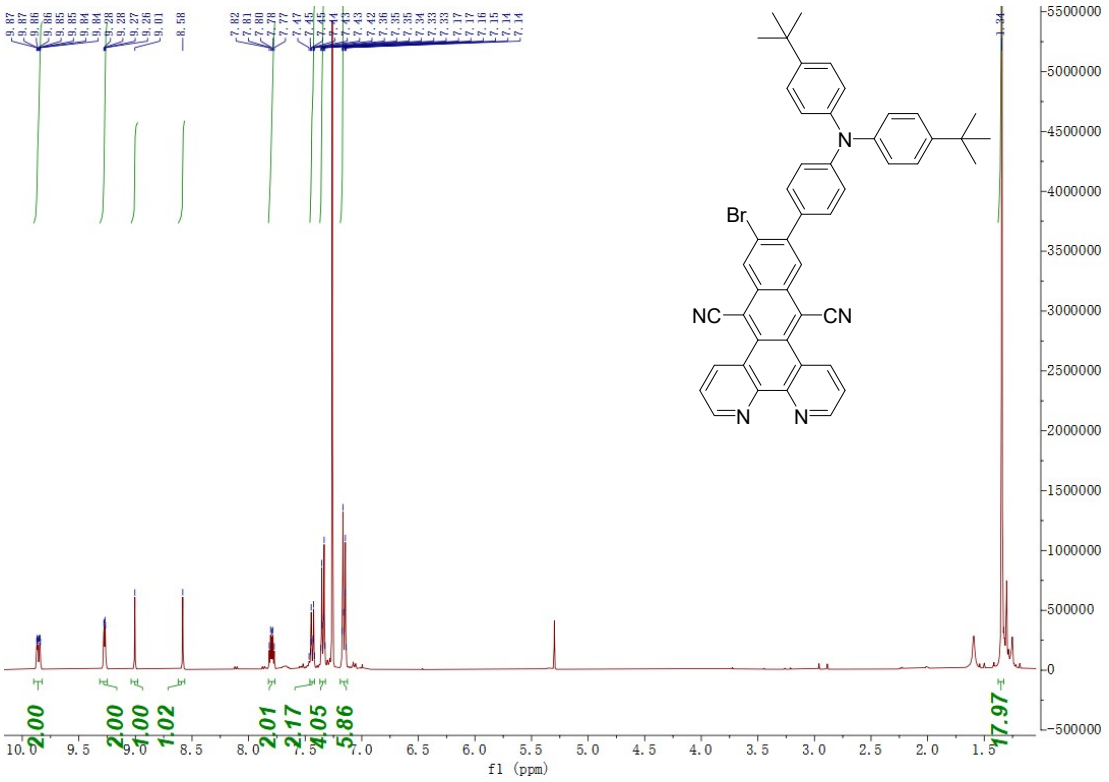

Figure S7 ^{1}H NMR spectrum ($CDCl_3$, 400 MHz) of TPA-1,10-2N-Br.

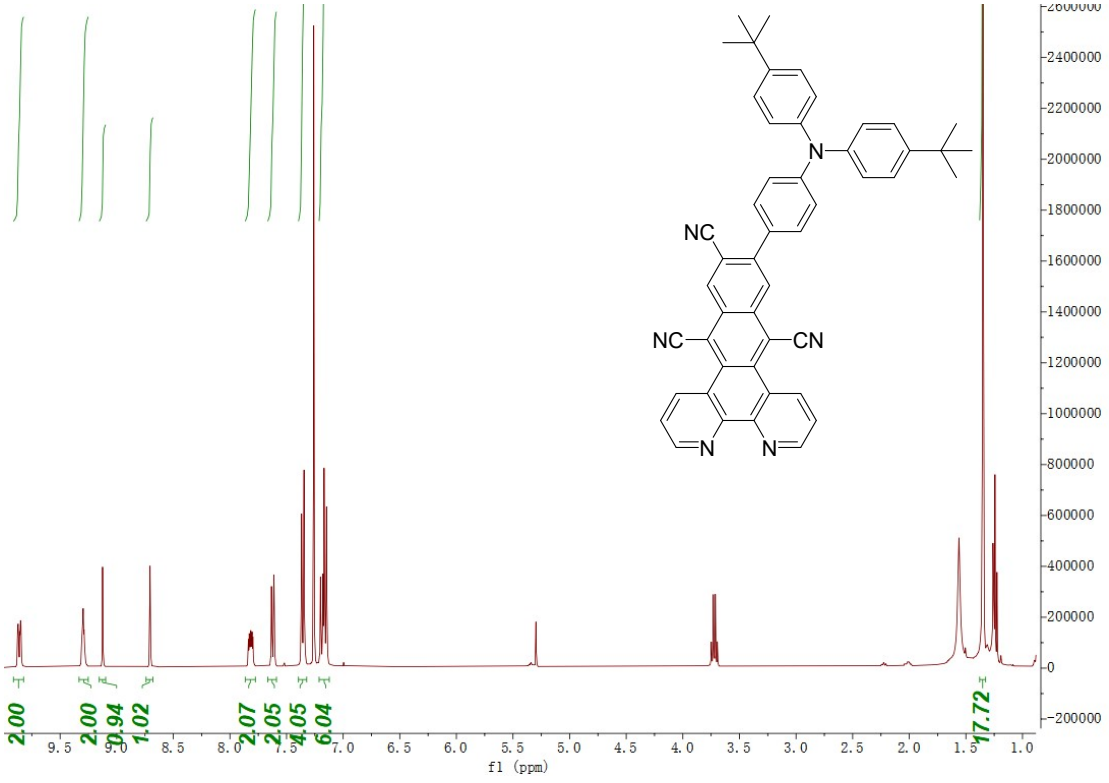

Figure S8 ^{1}H NMR spectrum ($CDCl_3$, 400 MHz) of TPA-1,10-2N.

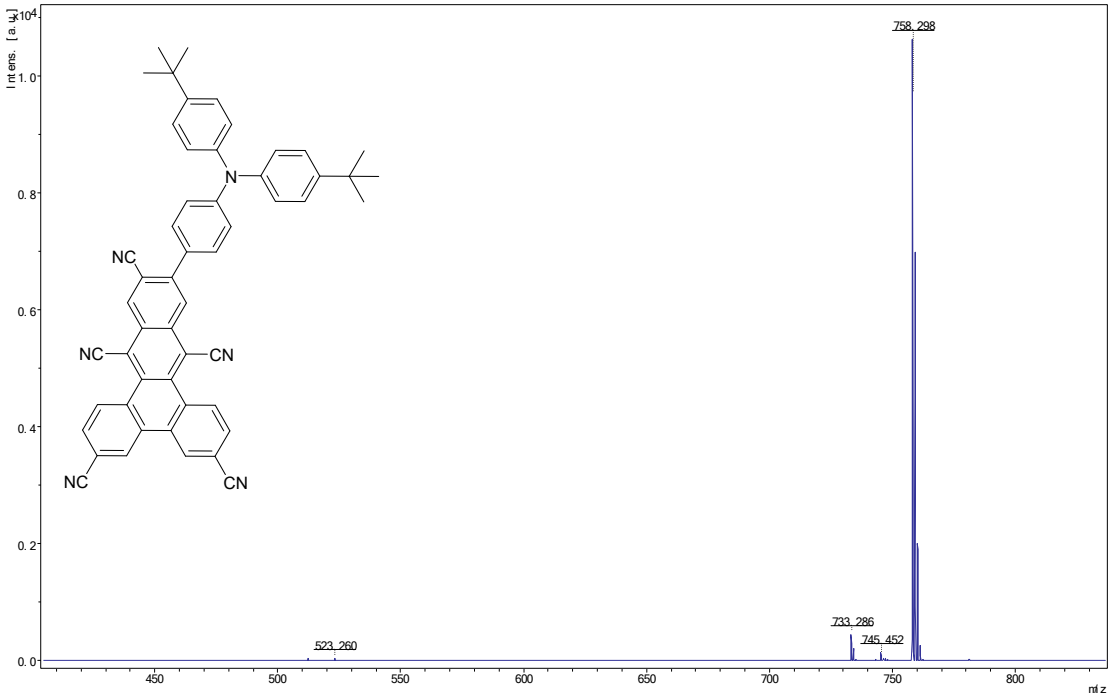

Figure S9 MALDI-TOF mass spectrum of TPA-5CN.

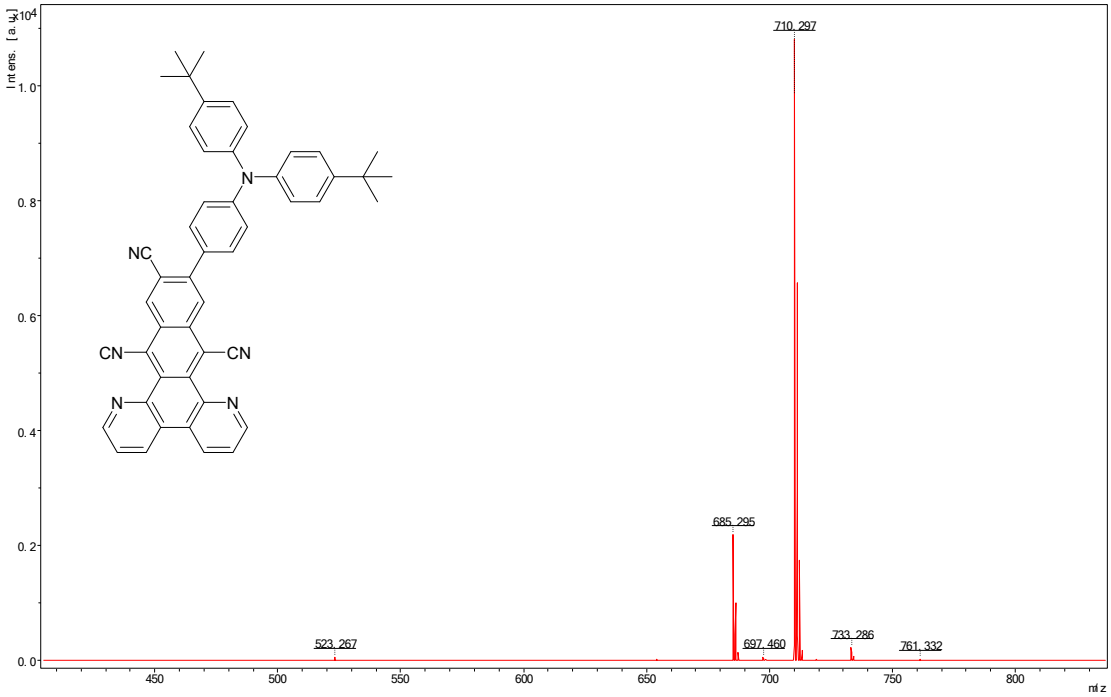

Figure S10 MALDI-TOF mass spectrum of TPA-2N.

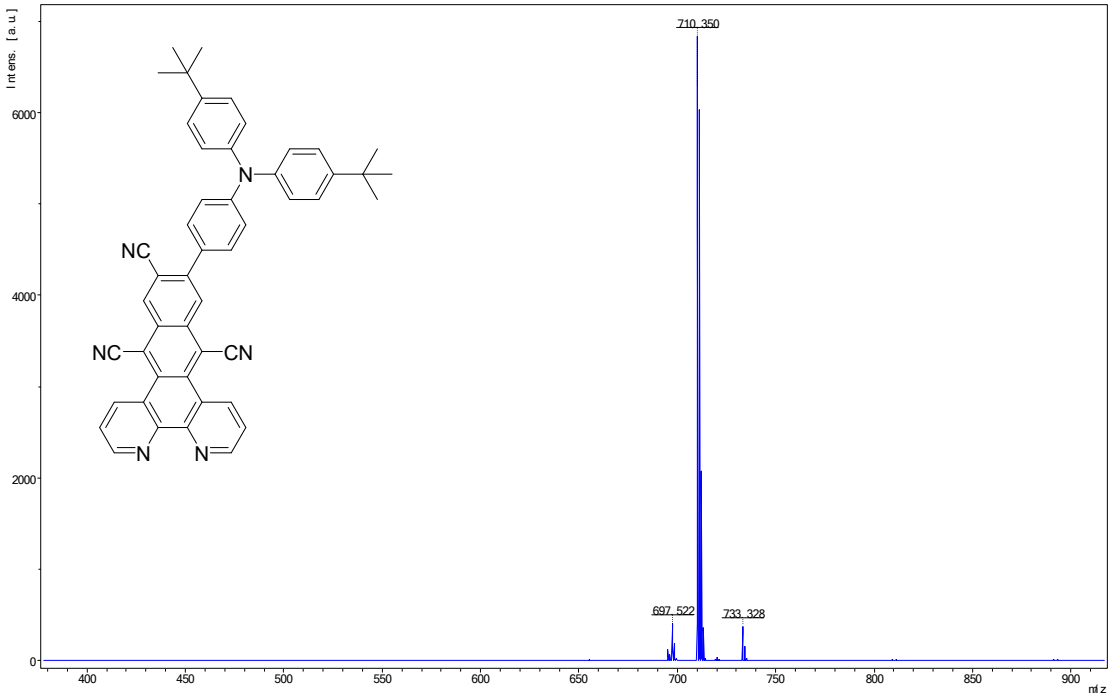

Figure S11 MALDI-TOF mass spectrum of TPA-1,10-2N.

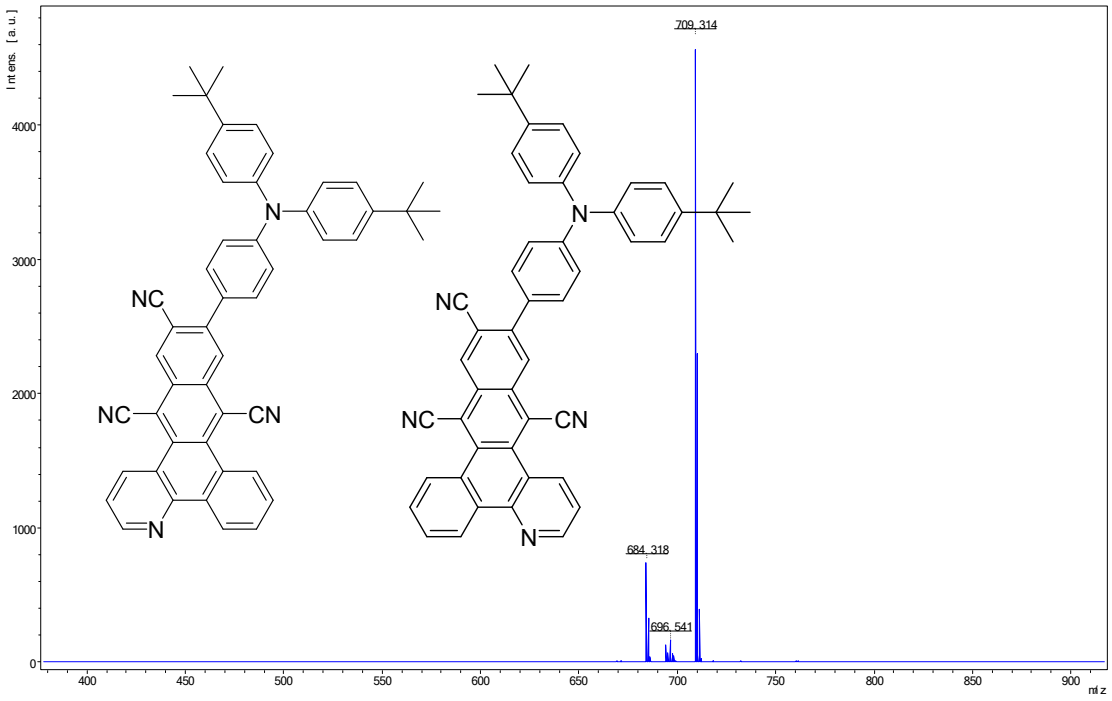

Figure S12 MALDI-TOF mass spectrum of TPA-N.

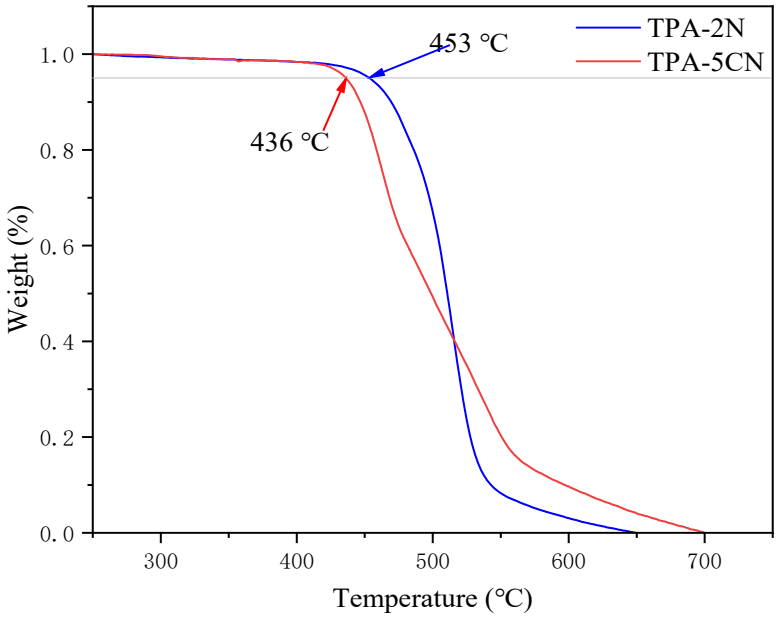

Figure S13 TGA curves of TPA-5CN and TPA-2N at a heating rate of 10 ℃/min under N_2.

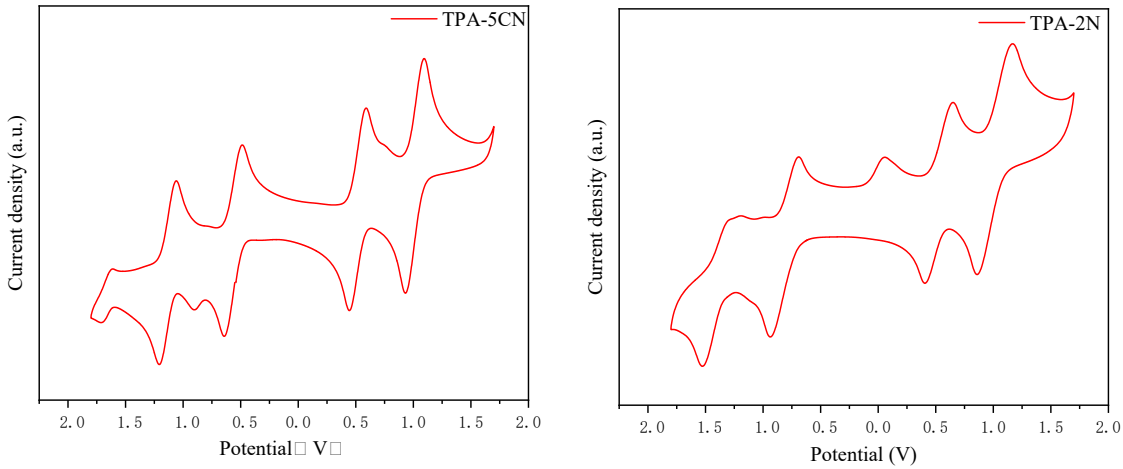

Figure S14 Cyclic voltammograms of TPA-5CN and TPA-2N.

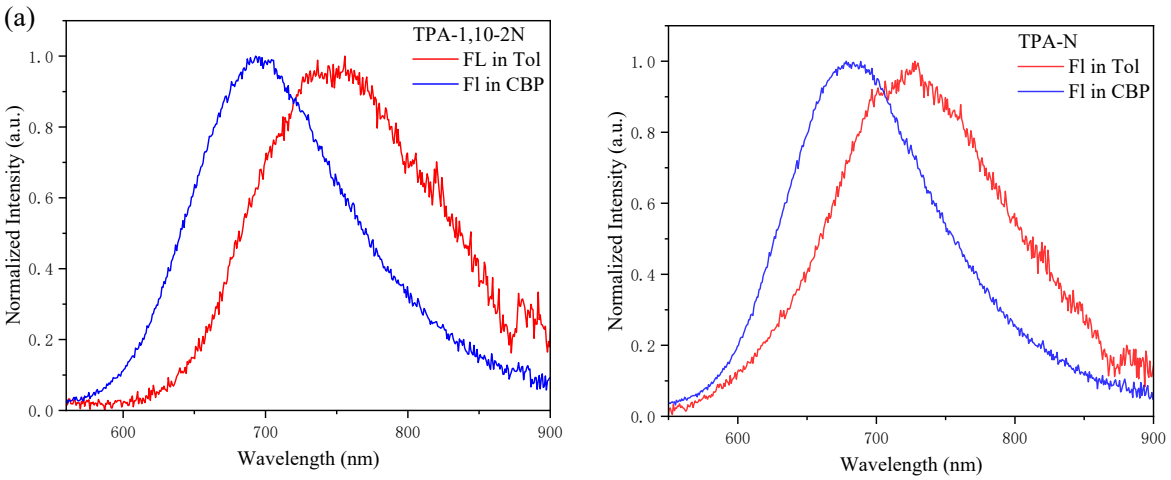

Figure S15 PL spectra of a dilute solution of TPA-1,10-2N (a) and TPA-N (b) in toluene (10^{-5} M) and doped films (3 wt%).

Table S1 Summary of the photoluminescence emission peaks of TPA-5CN, TPA-2N, TPA-1,10-2N, TPA-N in toluene and CBP doped films.

Compounds	λ_{em}^{tol} a) (nm)	λ_{em}^{film} b) (nm)	$\Delta\lambda$ (nm) b)
TPA-5CN	822	751	71
TPA-2N	698	670	28
TPA-1,10-2N	749	695	54
TPA-N	729	681	48

a) Measured in toluene solution (10^{-5} M) at 298 K.

b) Measured in doped films (3 wt% in CBP) at 298 K.

c) $\Delta\lambda = \lambda_{em}^{tol} - \lambda_{em}^{film}$.

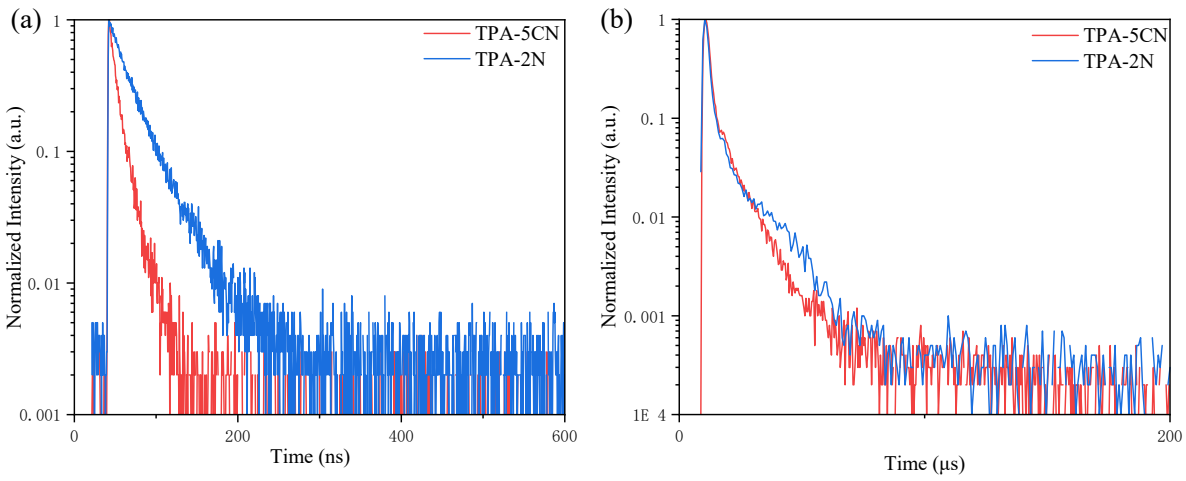

Figure S16　Transient PL decay curves of PF (a) and DF (b) components for TPA-5CN and TPA-2N in 3 wt% doped CBP films at 298 K.

Table S2 Photophysical characteristics of TPA-5CN and TPA-2N in CBP (3 wt% doped film).

Compound	Φ_{PL} [%]	Φ_F/Φ_{TADF} [%]	τ_F [ns]	τ_{TADF} [μs]	k_F [$10^7 s^{-1}$]	k_{IC} [$10^7 s^{-1}$]	k_{ISC} [$10^7 s^{-1}$]	k_{TADF} [$10^5 s^{-1}$]	k_{RISC} [$10^4 s^{-1}$]	Φ_{ISC} [%]
TPA-5CN	20.0	5.42/14.58	11.04	4.34	0.49	1.96	6.60	0.46	0.92	72.9
TPA-2N	64.5	30.34/34.16	27.86	5.29	1.09	0.60	1.90	1.22	7.85	53.0

a) Measured at 298 K.

$\mathbf{\Phi_{PL}}$ is the total fluorescence quantum yield; $\mathbf{\Phi_F}$ is the prompt fluorescent component of $\mathbf{\Phi_{PL}}$; $\mathbf{\Phi_{TADF}}$ is the delayed fluorescent component of $\mathbf{\Phi_{PL}}$; $\mathbf{\tau_F}$ is the lifetime of prompt fluorescent; $\mathbf{\tau_{TADF}}$ is the lifetime of TADF; $\mathbf{k_F}$ is the rate constant of fluorescent; $\mathbf{k_{IC}}$ is the rate constant of internal conversion; $\mathbf{k_{TADF}}$, $\mathbf{k_{ISC}}$, $\mathbf{k_{RISC}}$ are the rate constants of TADF, intersystem crossing and reverse intersystem crossing, respectively; $\mathbf{\Phi_{ISC}}$ and $\mathbf{\Phi_{RISC}}$ are the quantum efficiencies of ISC and RISC process, respectively.

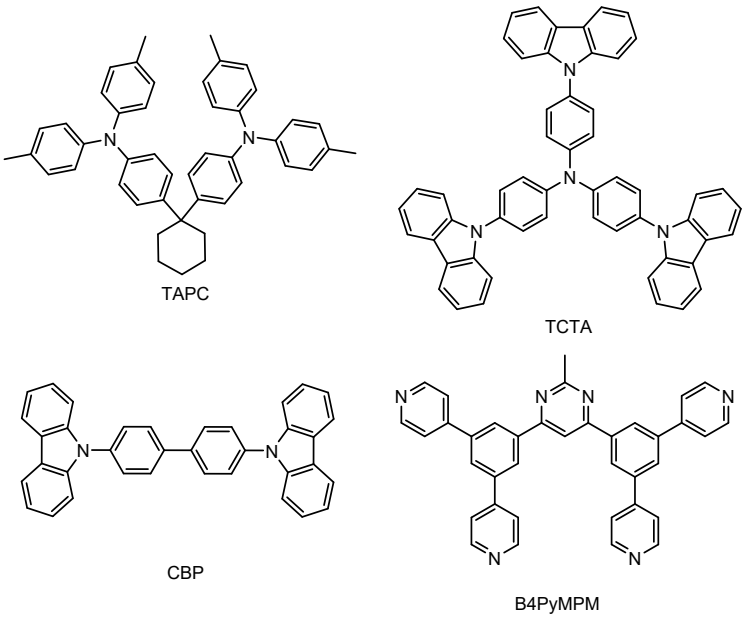

Figure S17 Molecular structures of the materials employed in the devices.

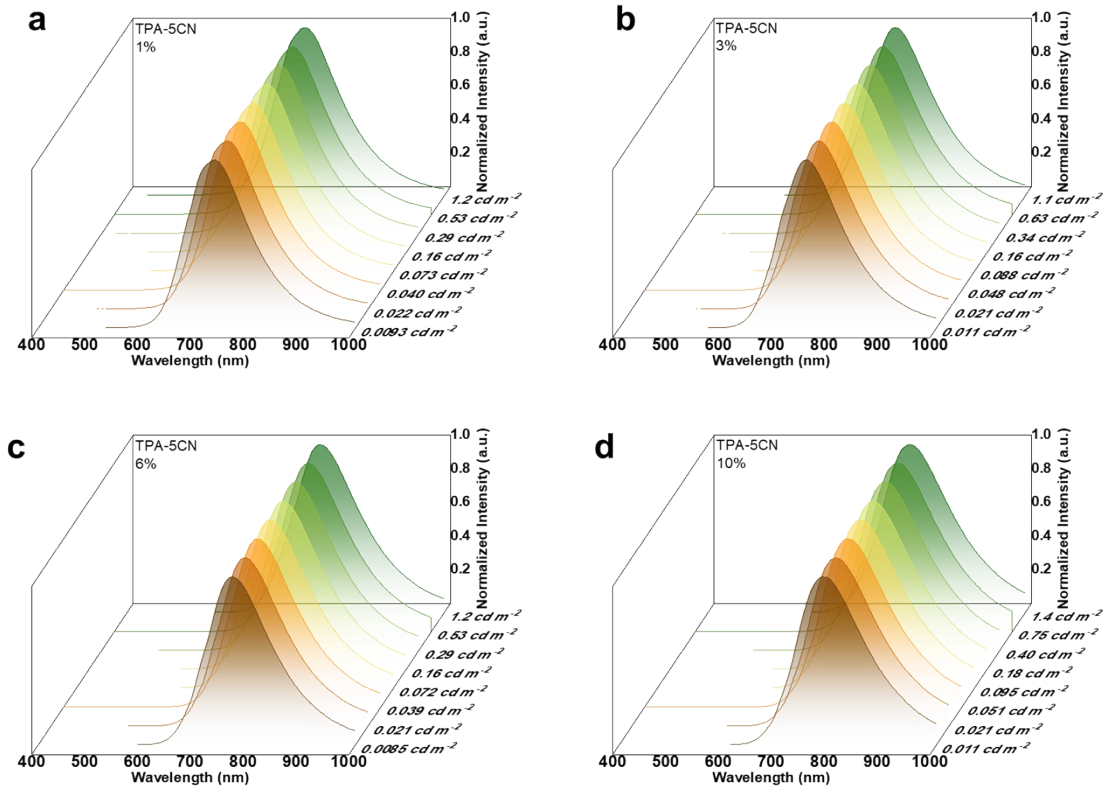

Figure 18. EL spectra of the TPA-5CN based devices at different luminance.

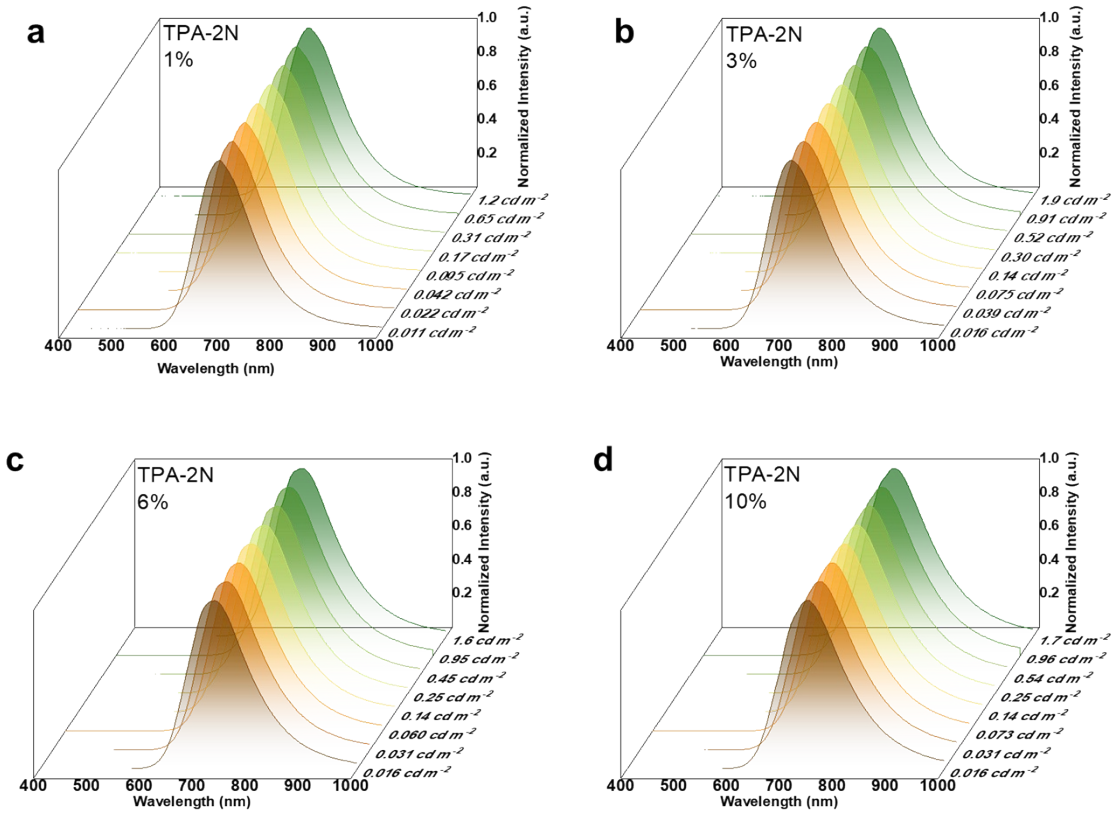

Figure S19. EL spectra of the TPA-2N based devices at different luminance.

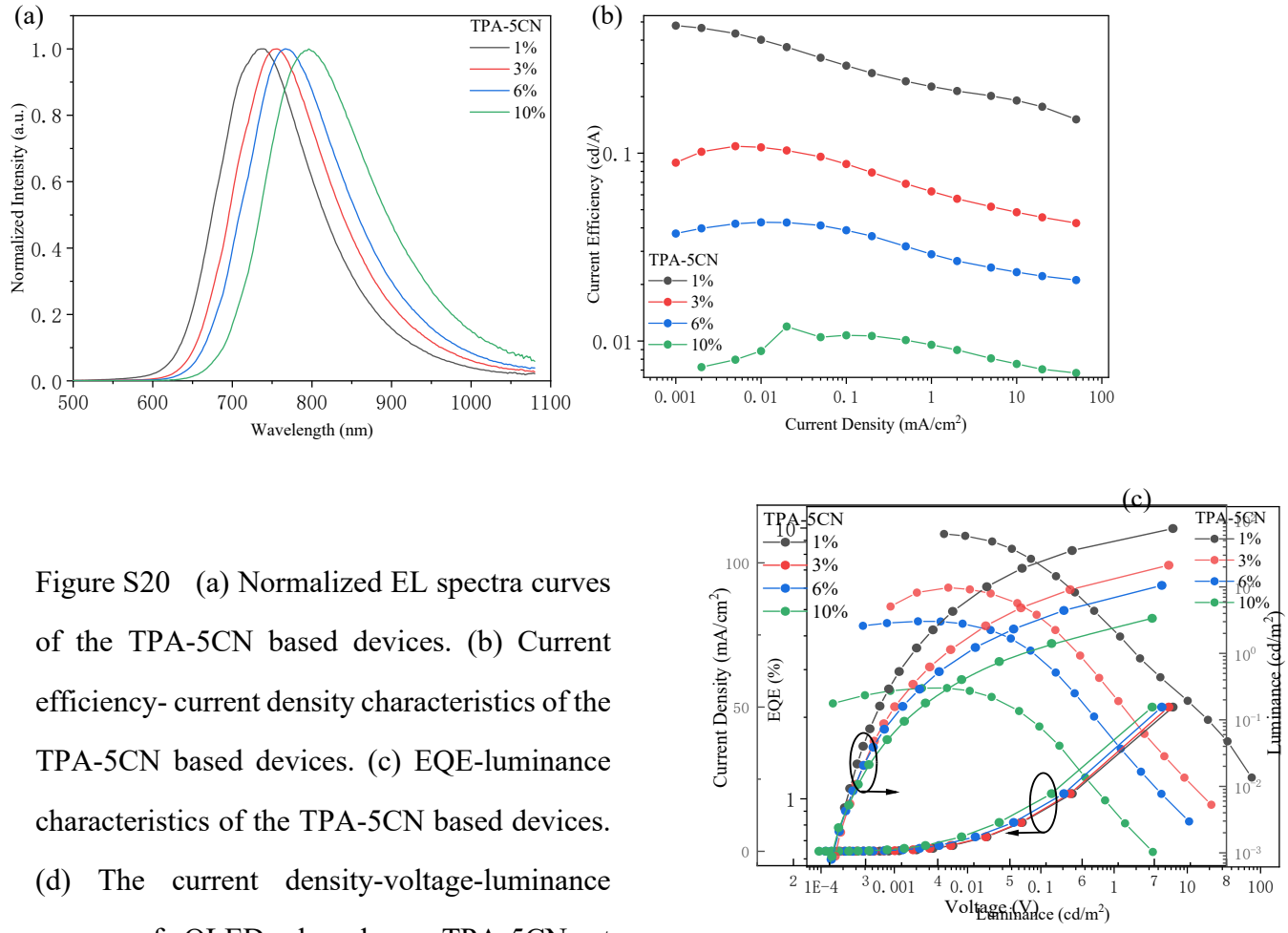

Figure S20 (a) Normalized EL spectra curves of the TPA-5CN based devices. (b) Current efficiency- current density characteristics of the TPA-5CN based devices. (c) EQE-luminance characteristics of the TPA-5CN based devices. (d) The current density-voltage-luminance curves of OLEDs based on TPA-5CN at different doping ratios.

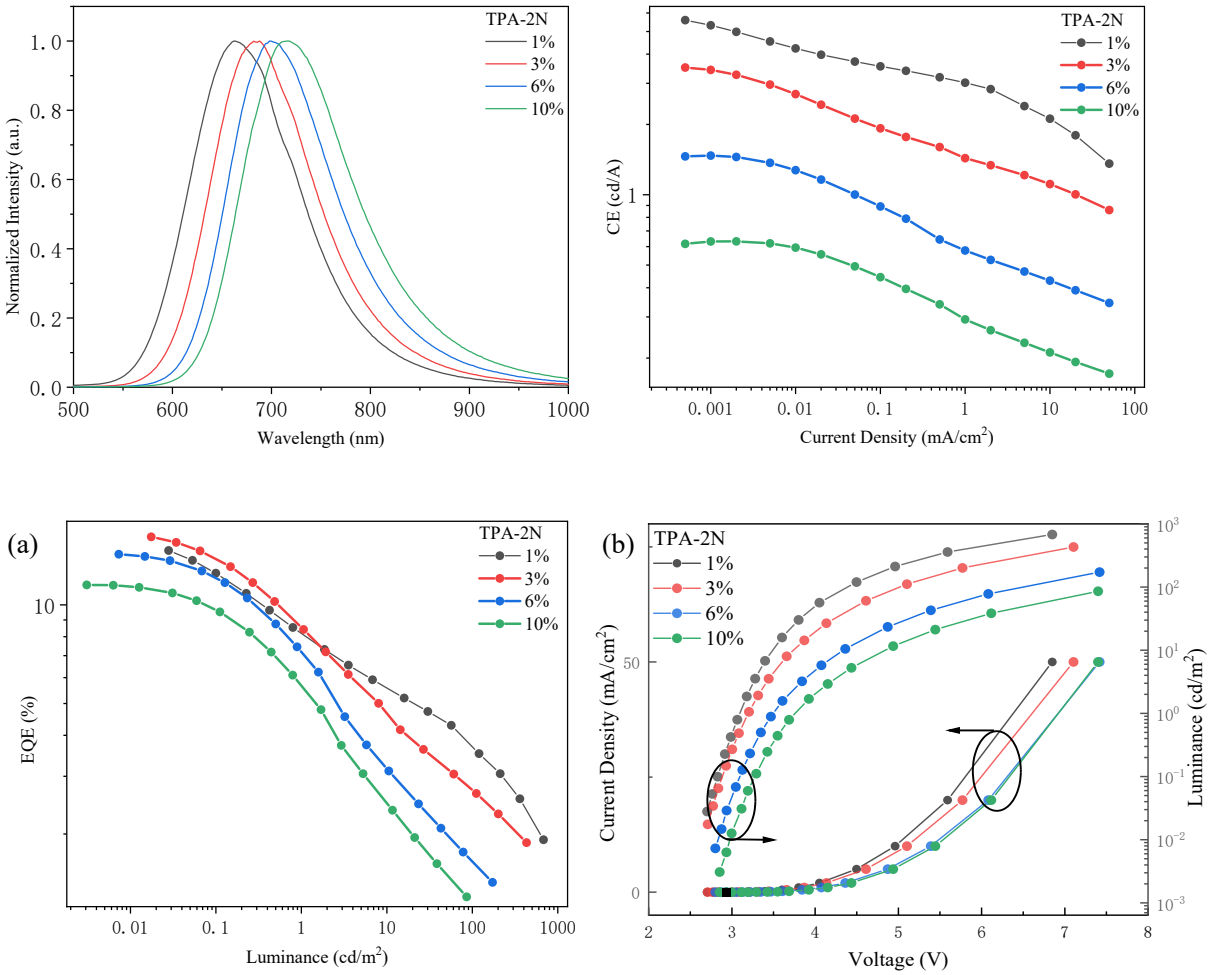

Figure S21 (a) Normalized EL spectra curves of the TPA-2N based devices. (b) Current efficiency- current density characteristics of the TPA-2N based devices. (c) EQE-luminance characteristics of the TPA-2N based devices. (d) The current density-voltage-luminance curves of OLEDs based on TPA-2N at different doping ratios.

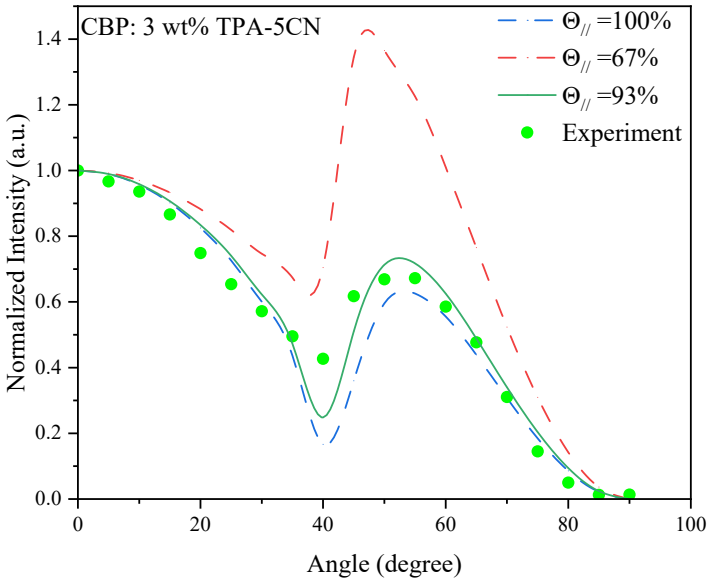

Figure S22 The angle-resolved and polarization-resolved PL intensity measurements of TPA-5CN in CBP doped films (3 wt%).

Table S3 EQE summary of representative doped NIR TADF-OLEDs with EL peaks from 770 to 800 nm

Emitters	EL peak (nm)	EQE_{max} (%)	References
TCN-TPA	775	3.2	3
	784	3.2	
	791	3.1	
	785	2.3	
1	788	0.4	4
	796	0.3	
	785	0.51	
AQTC-DTPA	770	1.51	5
	788	0.76	
DCzPBBT	772	4.06	6
	777	3.65	
This work	766	4.52	
	796	2.56	

References

[1] Frisch, M. J.; Trucks, G. W.; Schlegel, H. B.; Scuseria, G. E.; Robb, M. A.; Cheeseman, J. R.; Scalmani, G.; Barone, V.; Petersson, G. A.; Nakatsuji, H.; et al. Gaussian 16, Revision A.03; Gaussian, Inc.: Wallingford, CT, 2016.

[2] T. Lu and F. Chen, *J. Comput. Chem*. 2012, **33**, 580.

[3] J. X. Liang, Y. K. Tang, X. F. Wang, K. Zhang, Y. W. Shih, C. H. Chen, T. L. Chiu, P. J. Li, J. H. Lee, C. K. Wang, C. C. Wu and J. Fan, *J. Mater. Chem. C*, 2023, **11**, 6981.

[4] H. Ye, D.H. Kim, X. Chen, A.S.D. Sandanayaka, J.U. Kim, E. Zaborova, G. Canard, Y. Tsuchiya, E.Y. Choi, J.W. Wu, F. Fages, J.-L. Bredas, A. D'Aléo, J.-C. Ribierre, C. Adachi, *Chem. Mater*. 2018, **30**, 6702.

[5] J.-F. Cheng, Z.-H. Pan, K. Zhang, Y. Zhao, C.-K. Wang, L. Ding, M.-K. Fung, J. Fan, *Chem. Eng. J*. 2022, **430**, 132744.

[6] Y.-Y. Chen, Y.-C. Kung, M. S. Wang, Y.-C. Lo, Y.-T. Chia, C.-K. Wang, D.-G. Chen, J.-T Cheng, P.-T. Chou, C. Wu, E. Li, B. Hu, W.-Y. Hung, K.-T. Wong, *Adv. Optical Mater*. 2024, **12**, 2303131.